

Risk-Aware Path Planning for Ground Vehicles using Occluded Aerial Images

Vishnu Dutt Sharma and Pratap Tokekari

Abstract—We consider scenarios where a ground vehicle plans its path using data gathered by an aerial vehicle. In the aerial images, navigable areas of the scene may be occluded due to obstacles. Naively planning paths using aerial images may result in longer paths as a conservative planner may try to avoid regions that are occluded. We propose a modular, deep learning-based framework that allows the robot to *predict* the existence of navigable areas in the occluded regions. Specifically, we use image inpainting methods to fill in parts of the areas that are potentially occluded, which can then be semantically segmented to determine navigability. We use supervised neural networks for both modules. However, these predictions may be incorrect. Therefore, we extract uncertainty in these predictions and use a risk-aware approach that takes these uncertainties into account for path planning. We compare modules in our approach with non-learning-based approaches to show the efficacy of the proposed framework through photo-realistic simulations. The modular pipeline allows further improvement in path planning and deployment in different settings.

I. INTRODUCTION

Navigation in unknown areas in scenarios such as disaster response and post-accident scene analysis can be difficult and risky for in-field human supervision. To reduce the threat to human life, a team of Unmanned Ground Vehicle (UGV) and Unmanned Aerial Vehicle (UAV) can be deployed for such tasks. In this setting, the UAV flies above the area, capturing overhead images, and prescribes a path for navigation to the UGV, similar to finding a route on Google Maps. However, unlike satellite images, which generate images with orthographic projection, a UAV flies at a much lower height and captures images with perspective projection. Thus, in the images captured by a UAV, objects closer to the UAV such as a building may occlude the useful part of the scene situated farther away, such as the road (Figure 1), making it difficult to identify a good path for UAV navigation. We focus on the scenarios where the UAV acts as a scout, and captures the images of environment, which are used later for UGV navigation or localization, [1], [2], [3], [4]. These images may not contain views from different locations to provide us an idea of what lies behind the occlusions, limiting the use of such images for path planning. Similar situations may arise when the UAV and UGV are not in direct communication and are controlled by different entities.

Here, the occluded areas are undesired objects and should be replaced with the underlying scene to improve the path planning. Effectively, we want to predict what lies behind

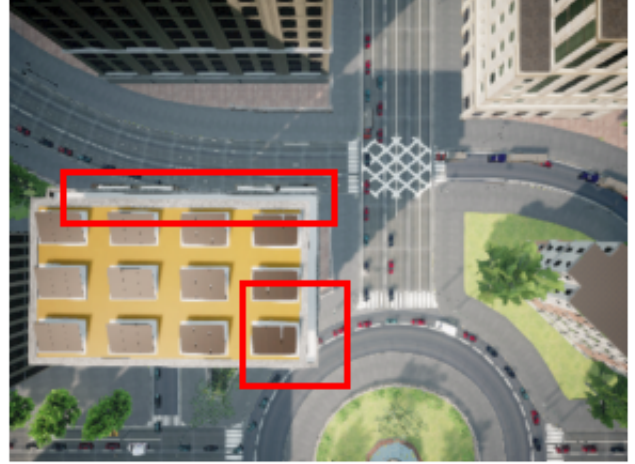


Fig. 1: Example of occlusions (shown in red rectangles) in an aerial image.

the occlusions. This approach would also eliminate the need of capturing images from multiple viewpoints. We propose using image inpainting for making these predictions over the likely navigable regions in the scene. Image inpainting is the process of filling a missing region in the image ideally with semantically correct information. The idea of replacing unwanted objects from the scene has been previously used in many areas (e.g. online photo touch-up [5], visual cultural heritage[6], etc.) and has advanced at a rapid pace in the past few years with the help of Generative Adversarial Networks (GANs) [7]. In this work, we propose to use this existing method for a robotic application and study the performance improvement brought in by it. An inpainting-based approach requires us to provide a mask specifying which parts of the image we wish to inpaint. As in our problem, the edges of the buildings and other obstacles occlude the road, we generate the mask as a block of pre-defined width, around the center of the road. The new image thus obtained contains the predictions over the masked parts. These predictions about what lies beneath the occlusions may not be perfect and thus they introduce uncertainty into the problem which needs to be taken into account while planning. Thus we use a risk-aware path planning approach which allows one to control their preference of risk-aversion and generates the path accordingly. Combining these steps, we propose a deep learning-assisted framework for planning a risk-aware path in aerial (overhead) images with occlusions, while allowing the user to choose the level of risk acceptable to them.

The authors are with Department of Computer Science, University of Maryland College Park, USA {vishnuds, tokekari}@umd.edu

This work is supported by the National Science Foundation under Grant No. 1943368

II. RELATED WORK

Replacing unwanted objects from the scene with background information is a well-known problem in computer vision. In these problems, we are generally given a mask denoting the unwanted regions along with the image. Prior to the shift towards machine learning, this problem has been addressed by techniques like Fast Marching [8] and Navier-Stokes method [9], where we grow the masked region based on information from the neighborhood pixels, texture-generation [10] and exemplar-based method [11]. In the past few years, deep learning has achieved tremendous success in different computer vision applications. Models like Deep Image Prior [12] show that the deep learning models are able to learn complex information about the image and can be used for super-resolution, denoising, and inpainting. As inpainting requires information synthesis, GANs [7] are generally used for this purpose, as they are capable of approximating highly complex non-linear functions. These GAN-based approaches generally use an image and a randomly generated mask as input and produce the original image. However, many of these approaches use regular shapes like rectangles for masking and therefore are not suitable for applications where mask shape is not controlled. Other GANs are trained on foreground objects masked and thus require manually masking the parts of the image to be precise. Liu et al. [13] propose a network that can overcome these problems and is able to inpaint images with irregular-shaped masks. We use this network for our application as we take an automated masking approach that can generate masks with irregular shapes.

Using inpainting, object removal can be posed as the process of masking the object of interest and inpainting over it. Objects in the images can be identified with object detection [14], optical flow [15], depth images [16], or even with GANs [17]. Becattini et al. [18] propose a semantic segmentation assisted masking followed by inpainting for removing dynamic obstacles on a road. We follow this strategy in our framework as semantic segmentation further helps us in path-planning by identifying the navigable areas. However, as most of the GANs are trained and tested on street-view images, object removal applications are also usually focused on those images. Work on inpainting aerial images is comparatively limited. Maalouf et al. [19] and Siravenha et al. [20] use image inpainting to remove clouds and shadows in satellite images, thus focusing on images with orthographic projection. Hsu et al. [21] propose an inpainting method aided by a super-resolution network showing its efficacy for front-facing aerial images. To the best of our knowledge, there is no work on inpainting for aerial overhead images with perspective projection, captured with a down-facing camera. A GANs have been shown to work with a variety of image data, we train a Partial Convolution based GAN [13], which allows inpainting irregular holes, on aerial images in our work.

After inpainting the occlusion in the image, the path planning can be done by applying semantic segmentation

over the modified image and extracting the information about the navigable areas. However, the inpainted areas are just predictions, and thus one should consider the risk associated with them while planning a path through them. Gal et al. [22], Tian et al. [23] and Loquercio et al.[24] present methods to extract uncertainty in predictions from deep learning model. Using the dropout-based approach [22], Sharma et al. [4] present a risk-aware planning framework for aerial images with an A* planner [25]. While their framework uses out-of-distribution images as the source of uncertainty in the evaluation, our framework introduces uncertainty by inpainting the images.

III. METHOD

An overview of our framework is given in Figure 2. Here, we extend the risk-aware pipeline proposed in [4] to also reason about occlusions. Specifically, we extend the pipeline to also have automated masking and inpainting modules. The resulting pipeline consists mainly of four steps described in the following subsections.

A. Mask Generation

This step generates a mask for identifying the areas that need to be modified/inpainted over. In this work, we treat the buildings near the road as the obstacle to be removed. Figure 3 shows the steps involved in this process. To identify such areas in the image, we first identify the center of the road and then mark all the buildings within a certain distance from the center as the obstacles to be removed. This marks the occluded areas near the road, which are likely to be navigable. The center of the road is found by performing semantic segmentation using a Bayesian SegNet [26] over the image and isolating the pixels pertaining to the road marker class to generate a binary map (Figure 3a). We generate another mask, marking the building in the scene using the segmentation (Figure 3b). The area surrounding the center is marked by performing dilation with a square mask of size 151×151 (Figure 3c). We use a square mask as most of the structures observed in aerial images have rectilinear shapes. In the final step, a bitwise-AND of the binary mask thus obtained and the mask for the buildings (Figure 3d). This last step is required to keep the masked area minimal for better inpainting.

B. Inpainting

Using the mask generated in the previous step as holes, we inpaint the original image to modify the areas of interest. As our masks are expected to be irregularly shaped, we use a partial convolutions-based GAN [13] which can fill irregular holes. While our image dataset was limited, random mask generation allows us to virtually train the model over a much larger number of images. We train this GAN over images where the road is not occluded, aiming to teach the GAN to complete a road if it is occluded by a mask.

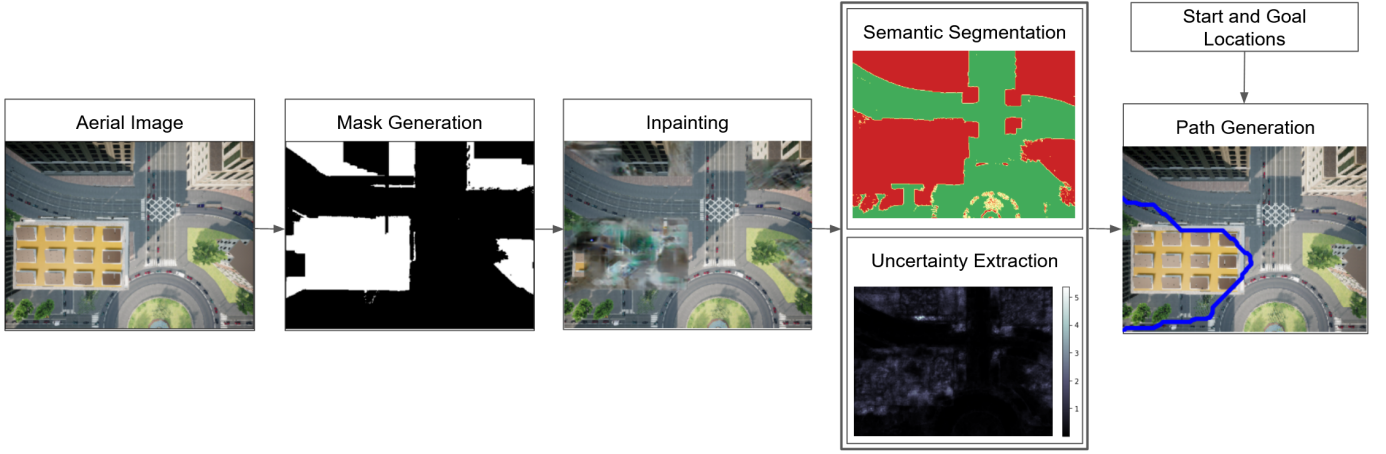


Fig. 2: Overview of the proposed framework. Given an aerial image, a mask is generated indicating the parts that need to be modified. Using the mask, the image is inpainted, and then semantic segmentation and uncertainty map are generated. A path-planner uses a combination of them to generate a risk-aware path.

C. Path Planning

We use A* search for planning the path between two points (pixels) on the image. The path generated depends on how much cost is assigned to each pixel. For risk-aware planning, we construct a cost matrix, that contains the cost of navigation for each pixel in the image, using two components as suggested by Sharma et al. [4]. The first component is the user-defined cost assigned to different classes in the semantic segmentation of the image. The second component quantifies the uncertainty in the segmentation prediction as the average variance in the predictions, i.e., $\text{Uncert}(l_x) = \frac{1}{K} \sum_k \text{Var}_n(P(l_x|x))$, where l_x is label assigned to the pixel under investigation, x is the image, K is the number of classes/labels, $\text{Var}_n(\cdot)$ is variance calculated over n samples. The cost matrix is obtained as follows:

$$\hat{C}(x) = C(l_x) + \lambda \cdot \text{Uncert}(l_x), \quad (1)$$

where $C(l_x)$ is the cost map denoting the cost assigned to the pixel l_x .

IV. EXPERIMENTS

Our framework uses two deep-learning models, a semantic segmentation model for mask and cost-matrix generation, and an image inpainting model for modifying the masked parts of the image. We use *CityEnviron* environment of AirSim [27] simulator to generate training and test images for each step. We use AirSim because it provides photo-realistic images, their semantic segmentation, and orthographic views. The image inpainting model [28] is trained over a set of images captured by flying the UAV on a path directly above the road, at heights of 30m, 70m, 100m, and 130m. We use 2248 images, splitting them with a ratio of 75:15:15 for training, validation, and test for the inpainting model. We also generate 1000 randomly placed rectangles of random sizes as masks, which can cover the road partially or completely, similar to a building top covering the road in the images. The model was trained for 10^6 epochs. We train the

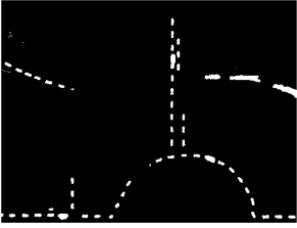
semantic segmentation model [29] to predict semantic labels from a specific height and use images captured at a height of 100m, capturing the entire *CityEnviron*. We train the segmentation model over 420 images, spitted into training, validation and, test sets in a ratio of 10:3:3, and use vertical and horizontal flipping for data augmentation. The ground truth labels consist of 11 classes including road, building, road markers, and trees.

As our framework is modular, we also compare the effects of non-learning-based approaches for masking and inpainting. For masking, we compare our automated masking method against manual masking. For inpainting, we study the effects of three other methods: (a) filling the masked areas with average values of pixels belonging to the road in the image, (b) replacing the masked areas with a road-like patch generated manually, and (c) using Navier-Stokes inpainting method. We refer to these as *mean-replacement*, *patch-replacement*, and *Navier-Stokes*, respectively.

For the path-planning step, we define the cost by categorizing the predicted semantic labels into two classes, (a) *navigable*, which contains roads and markers only and is assigned a cost of 1, and (b) *non-navigable* which contains all other labels has a cost of 10. For calculating the variance, we generate 20 samples. We try multiple values of λ to show paths generated for different levels of risk-aversion. The effect of λ on path planning is quantified as *surprise*, which is equal to the cost of traversing the path on the cost matrix for ground truth minus cost of traversal of this path on the cost matrix on the inpainted image, normalized by the length of the path, i.e.,

$$\text{surprise} = \frac{\sum_{l_x \in \text{path}} C_{\text{true}}(l_x) - C_{\text{pred}}(l_x)}{\text{length}(\text{path})}, \quad (2)$$

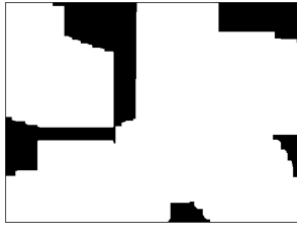
where *path* is the path over pixels as prescribed by the planner, and C_{true} and C_{pred} are the cost matrix generated over semantic segmentation outputs from the approximated ground truth (shown in Figure 5b) and inpainted images,



(a) Road markers



(b) Buildings



(c) Dilated road markers



(d) Final mask ($b \cdot c$)

Fig. 3: Stages of mask generation. A dilation kernel of size 121×121 is used here.

respectively. A higher surprise indicates that a larger part of the path passes through risky regions. As surprise depends on the start and goal locations in the scene, we pick 5 locations on the scene image, as shown in Figure 4a with red dots and find surprise over the 10 resulting source-goal combinations. We report the statistics for both the original scene including occlusions and the inpainted image generated by our framework.

V. RESULTS

In this section, we first compare the proposed framework against non-learning-based methods for masking and inpainting. Then we present the results of path-planning with our approach and the conclusions drawn from our observations. We use the image shown in Figure 4 as the reference for all the results. As *CityEnviron* does not allow removing objects from the scene, we captured multiple orthographic images, stacked them together and, warped to get an approximate scene and semantic segmentation (shown in Figure 5) to act as the ground truth for the reference scene.

A. Masking

Figure 6 shows the results for manual and automated masking. The last row shows the result of segmentation over the inpainted image. The masked areas are shown with black patches. For automated masking, we compare the effect of using a small square kernel (121×121) and a large square kernel (151×151) for dilation. We specifically focus on the orange building in the left part of the scene for this discussion. The inpainted areas in the image look more regular for manual masking and the growth in the navigable regions is condensed in regions close to the road for manual masking. But, automated kernels result in comparatively more continuous navigable regions in the segmentation outputs. Mask produced by the small kernel



(a) Scene



(b) Segmentation

Fig. 4: Reference input and ground truth semantic segmentation with perspective projection. The red dots show the locations used for calculating surprise.



(a) Scene



(b) Segmentation

Fig. 5: Orthographic projection (approximate) of the reference image and the corresponding ground truth semantic segmentation.

is closer to the manual mask in form. However, since road markers get occluded by the top of the building (shown in Figure 3a), it leaves some portion of the building unmarked. Thus, we use a larger kernel that masks all the edges of the building. It also masks other occlusions in the scene (top and right edges of the scene) better than the small kernel, making it more suitable when there are multiple occluded regions in the scene.

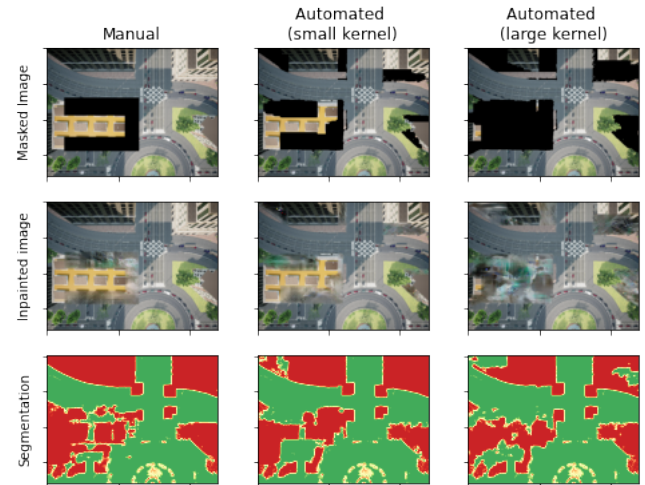


Fig. 6: Comparison of non-learning and learning-based approaches for masking.

B. Inpainting

For these experiments, we use the automated mask with a dilation kernel of size 151×151 (i.e. large kernel), as depicted in Figure 6. The results are shown in Figure 7. Mean-replacement generates segmentation almost similar to the reference (Figure 4b) and thus is not helpful for our purpose. Patch-replacement makes most of the building navigable as expected, as we are replacing the mask with pixels belonging to a navigable class. Navier-Stokes inpainting results in very smooth inpainting, but the semantic segmentation sees a limited growth in the navigable region. Inpainting with GAN is comparatively more controlled and accurate in predicting the navigable areas. In each of these cases, we expect high uncertainty in the masked areas. Mean-replacement has a very low uncertainty in these areas, which further makes it unsuitable. Inpainting has a slightly higher uncertainty in the masked regions, which makes it more appropriate for the risk-aware path planning problem.

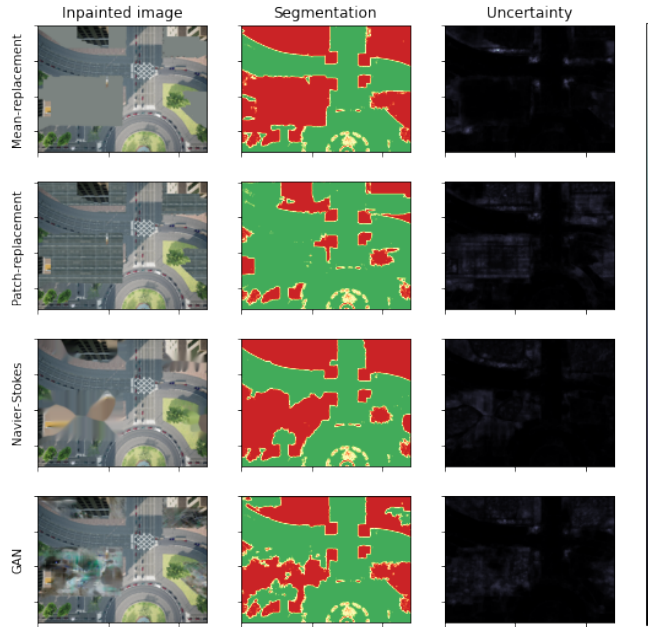


Fig. 7: Comparison of approaches for inpainting.

C. Path Planning

Images in Figure 9 show the paths generated for different values of λ when we use the original image for risk-aware planning and when we use the proposed framework. For higher values of λ , the path proposed tries to keep away from the building as it was masked, resulting in higher prediction variance. A comparison of surprise calculated over the two inputs, shown in Figure 8, brings forth the effect of risk-awareness when over the predictions made by the inpainting step. On average, the inpainted image results in slightly lesser surprise than the original image, as inpainting allows the path to go through the occluded, navigable areas. Both of them have a higher variance for smaller λ s as it encourages them to pass through uncertain regions for a

shorter path. As we increase the λ , the path planner gets risk-averse and hence passes through the regions which have a high chance of being navigable. In these cases, the surprise for both gets close to zero and has a much smaller variance. We wish to emphasize here that the effect of λ is related to the cost of the classes. For a very high difference in the cost of navigable and non-navigable classes, the effect of lambda may get diluted.

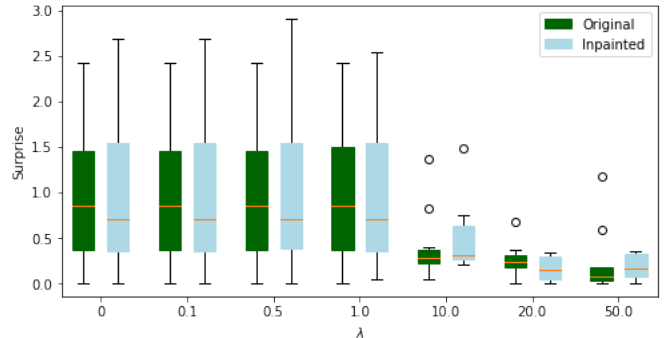


Fig. 8: Surprise for various λ s over original and inpainted images. Cost of passing through the navigable and non-navigable pixels is 1 and 10, respectively.

VI. CONCLUSIONS

In this work, we propose a modular, risk-aware path planning framework in aerial images containing occlusions. We leverage deep learning techniques of image inpainting and semantic segmentation to identify occluded areas, replace them with what might lie behind beneath, and plan a path considering the uncertainty that these predictions introduce. We compare the steps of our framework with non-learning-based methods to justify the need for learning-based solutions. Finally, we qualitatively and quantitatively compare the path planning results to show the advantage of our approach.

Our observations on experiments on masking show that while automated masking may be desired to avoid the requirement of human intervention, it may need to be replaced with manual masking for applications where occlusion hampers the process of masking. We present a simple approach for automated masking in this work and it has the scope of further improvement. We also wish to point out that our inpainting model was trained on a smaller set of images than generally used for such models and thus can be further improved to produce more real-looking results.

The modular design opens multiple avenues for future work, including improvements in efficiency and accuracy of the individual steps using other models or with larger data. The obstacle detection and inpainting steps may be replaced with an end-to-end model as well. While we present the framework for aerial images, it can be used for street-view images with the appropriate substitutions, without the need of training models from scratch due to the abundance of pre-trained models for such images. Analysis of the effects of

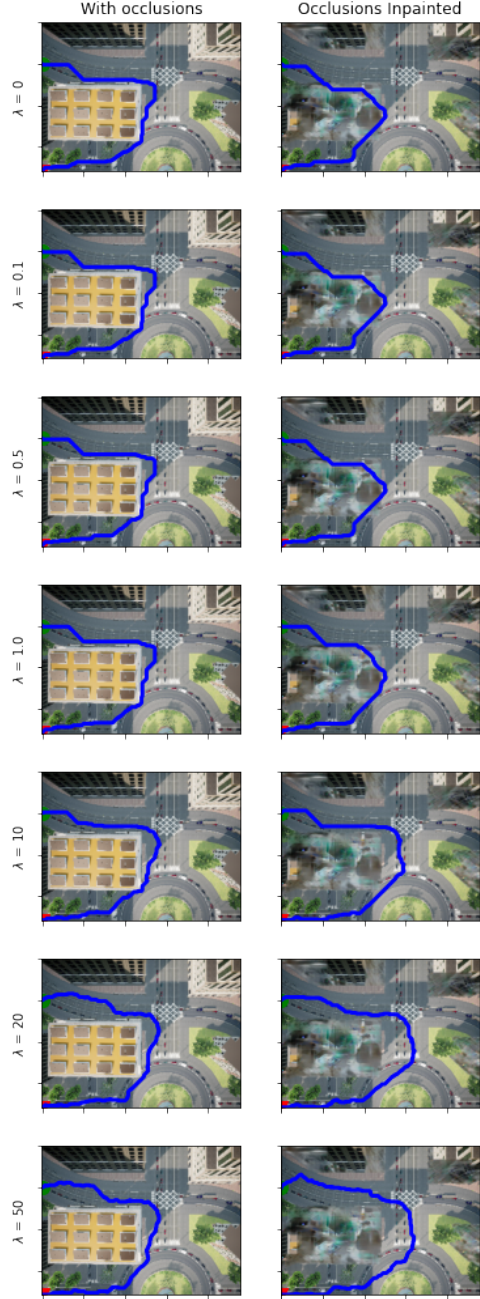


Fig. 9: Comparison of paths predicted for various λ s for the image with occlusions and the inpainted image

other uncertainty metrics is another interesting direction for further study.

REFERENCES

- [1] G. Christie, A. Shoemaker, K. Kochersberger, P. Tokekar, L. McLean, and A. Leonessa, "Radiation search operations using scene understanding with autonomous uav and ugv," *Journal of Field Robotics*, vol. 34, no. 8, pp. 1450–1468, 2017.
- [2] D. Dixit and P. Tokekar, "Evaluation of cross-view matching to improve ground vehicle localization with aerial perception," *arXiv preprint arXiv:2003.06515*, 2020.
- [3] M. Toubeh and P. Tokekar, "Risk-aware planning by confidence estimation using deep learning-based perception," *arXiv preprint arXiv:1910.00101*, 2019.
- [4] V. Sharma, M. Toubeh, L. Zhou, and P. Tokekar, "Risk-aware planning and assignment for ground vehicles using uncertain perception from aerial vehicles," in *Proceedings of the IEEE/RSJ International Conference on Intelligent Robots and Systems (IROS)*, 2020.
- [5] O. Whyte, J. Sivic, and A. Zisserman, "Get out of my picture! internet-based inpainting," in *BMVC*, vol. 2, no. 4, 2009, p. 5.
- [6] N. H. Jboor, A. Belhi, A. K. Al-Ali, A. Bouras, and A. Jaoua, "Towards an inpainting framework for visual cultural heritage," in *2019 IEEE Jordan International Joint Conference on Electrical Engineering and Information Technology (JEEIT)*. IEEE, 2019, pp. 602–607.
- [7] I. J. Goodfellow, J. Pouget-Abadie, M. Mirza, B. Xu, D. Warde-Farley, S. Ozair, A. Courville, and Y. Bengio, "Generative adversarial networks," *arXiv preprint arXiv:1406.2661*, 2014.
- [8] A. Telea, "An image inpainting technique based on the fast marching method," *Journal of graphics tools*, vol. 9, no. 1, pp. 23–34, 2004.
- [9] M. Bertalmio, A. L. Bertozzi, and G. Sapiro, "Navier-stokes, fluid dynamics, and image and video inpainting," in *Proceedings of the 2001 IEEE Computer Society Conference on Computer Vision and Pattern Recognition. CVPR 2001*, vol. 1. IEEE, 2001, pp. I–I.
- [10] S. D. Rane, G. Sapiro, and M. Bertalmio, "Structure and texture filling-in of missing image blocks in wireless transmission and compression applications," *IEEE transactions on image processing*, vol. 12, no. 3, pp. 296–303, 2003.
- [11] A. V. Pinjarkar and D. Tuptewar, "Robust exemplar-based image and video inpainting for object removal and region filling," in *Computing, Communication and Signal Processing*. Springer, 2019, pp. 817–825.
- [12] D. Ulyanov, A. Vedaldi, and V. Lempitsky, "Deep image prior," in *Proceedings of the IEEE conference on computer vision and pattern recognition*, 2018, pp. 9446–9454.
- [13] G. Liu, F. A. Reda, K. J. Shih, T.-C. Wang, A. Tao, and B. Catanzaro, "Image inpainting for irregular holes using partial convolutions," in *Proceedings of the European Conference on Computer Vision (ECCV)*, 2018, pp. 85–100.
- [14] O. Angah and A. Y. Chen, "Removal of occluding construction workers in job site image data using u-net based context encoders," *Automation in Construction*, vol. 119, p. 103332, 2020.
- [15] Y. Hirohashi, K. Narioka, M. Suganuma, X. Liu, Y. Tamatsu, and T. Okatani, "Removal of image obstacles for vehicle-mounted surrounding monitoring cameras by real-time video inpainting," in *Proceedings of the IEEE/CVF Conference on Computer Vision and Pattern Recognition Workshops*, 2020, pp. 214–215.
- [16] L. Wang, S. Xie, W. Xu, B. Yao, J. Cui, Q. Liu, and Z. Zhou, "Human point cloud inpainting for industrial human-robot collaboration using deep generative model," in *International Manufacturing Science and Engineering Conference*, vol. 84263. American Society of Mechanical Engineers, 2020, p. V002T07A023.
- [17] J. Pyo, Y. G. Rocha, A. Ghosh, K. Lee, G. In, and T. Kuc, "Object removal and inpainting from image using combined gans," in *2020 20th International Conference on Control, Automation and Systems (ICCAS)*. IEEE, 2020, pp. 1116–1119.
- [18] F. Becattini, L. Berlincioni, L. Galteri, L. Seidenari, and A. Bimbo, "Semantic road layout understanding by generative adversarial inpainting," *CoRR*, 2018.
- [19] A. Maalouf, P. Carré, B. Augereau, and C. Fernandez-Maloigne, "A bandelet-based inpainting technique for clouds removal from remotely sensed images," *IEEE transactions on geoscience and remote sensing*, vol. 47, no. 7, pp. 2363–2371, 2009.
- [20] A. C. Siravenha, D. Sousa, A. Bispo, and E. Pelaes, "Evaluating inpainting methods to the satellite images clouds and shadows removing," in *International Conference on Signal Processing, Image Processing, and Pattern Recognition*. Springer, 2011, pp. 56–65.
- [21] C. Hsu, F. Chen, and G. Wang, "High-resolution image inpainting through multiple deep networks," in *2017 International Conference on Vision, Image and Signal Processing (ICVISP)*. IEEE, 2017, pp. 76–81.
- [22] Y. Gal and Z. Ghahramani, "Dropout as a bayesian approximation: Representing model uncertainty in deep learning," in *international conference on machine learning*. PMLR, 2016, pp. 1050–1059.
- [23] J. Tian, W. Cheung, N. Glaser, Y.-C. Liu, and Z. Kira, "Uno: Uncertainty-aware noisy-or multimodal fusion for unanticipated input degradation," in *2020 IEEE International Conference on Robotics and Automation (ICRA)*. IEEE, 2020, pp. 5716–5723.
- [24] A. Loquercio, M. Segu, and D. Scaramuzza, "A general framework for uncertainty estimation in deep learning," *IEEE Robotics and Automation Letters*, vol. 5, no. 2, pp. 3153–3160, 2020.

- [25] P. E. Hart, N. J. Nilsson, and B. Raphael, “A formal basis for the heuristic determination of minimum cost paths,” *IEEE transactions on Systems Science and Cybernetics*, vol. 4, no. 2, pp. 100–107, 1968.
- [26] A. Kendall, V. Badrinarayanan, and R. Cipolla, “Bayesian segnet: Model uncertainty in deep convolutional encoder-decoder architectures for scene understanding,” 2016.
- [27] S. Shah, D. Dey, C. Lovett, and A. Kapoor, “Airsim: High-fidelity visual and physical simulation for autonomous vehicles,” in *Field and service robotics*. Springer, 2018, pp. 621–635.
- [28] N. Inoue, S. Seitz, and V. M. Gonzalez, “Pytorch implementation of image inpainting for irregular holes using partial convolutions.” <https://github.com/naoto0804/pytorch-inpainting-with-partial-conv>, 2018.
- [29] M. P. Shah, “Semantic segmentation architectures implemented in pytorch.” <https://github.com/meetshah1995/pytorch-semseg>, 2017.